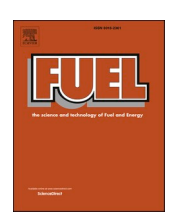


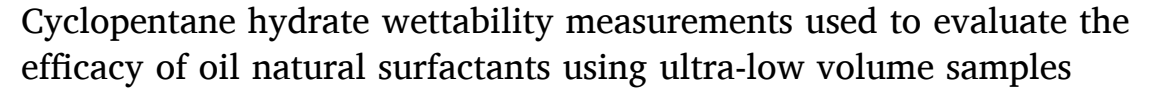
Contents lists available at ScienceDirect

Fuel

journal homepage: www.elsevier.com/locate/fuel



Full Length Article



Hannah M. Stoner, Jefferson Moak, Jose G. Delgado-Linares, Carolyn A. Koh

Center for Hydrate Research, Colorado School of Mines - Department of Chemical and Biological Engineering, 1613 Illinois St, Golden, CO 80401, USA



ARTICLE INFO

Keywords: Clathrate hydrates Cyclopentane Contact angle Oil Asphaltenes Film growth

ABSTRACT

Hydrate surface wettability is a fundamental aspect to better understand agglomeration present in oil bearing petroleum pipelines. Coupling these measurements with hydrate film growth gives further information on kinetic effects that may also be present from natural surfactants in different oils. In situ measurements of wettability (quantified by the contact angle) and film growth rates were performed on cyclopentane hydrate surfaces at atmospheric pressure and subcooling of 4 °C. Contact angle and film growth results were obtained for the baseline system (pure cyclopentane), one model oil, and seventeen natural oils (diluted to 0.02 vol% in cyclopentane). Results showed a wide variety of contact angles and film growth values where higher asphaltene contents in the oils corresponded to higher contact angles and lower film growth rates, thought to be from better alignment of natural surfactant molecules at the hydrate/hydrocarbon interface. It was also shown for select oils that increasing the oil concentration in the cyclopentane increases the contact angle and decreases the film growth rate compared to the baseline system. For select oils that had higher contact angles, increasing the water content of the system decreases their contact angle and film growth compared to the baseline system. Isolating different oil fractions for select oils also shows which fractions tend to play a larger role in wettability behavior. Typically, the fractions with more surface active components (asphaltene and resins) are shown to contribute to the higher contact angle and slower film growth rates for select oils. Evidence of the competition between film growth and capillary suction of water into the hydrate has been shown, and a mechanistic breakdown of three different transient scenarios has been proposed. Each of these observed interfacial behaviors gives information on what can be expected from larger scale phenomena, including hydrate agglomeration, with very small oil samples.

1. Introduction

Gas hydrates are solid inclusion compounds with a hydrogen bonded cage structure of water molecules that trap small guest molecules, discovered in 1811 by Sir Humphry Davy [1]. Generally, hydrates form under high pressure and low temperature conditions. This makes it possible for their formation naturally [2–6] and in laboratory and industrial applications including desalination [7,8], gas or liquid separation [9,10], and production [11,12], or storage [13,14]. Hydrates also form in oil and gas pipelines [15] and are considered an acute problem facing the oil and gas industry today. Hydrate unit cells are comprised of different molecular cages (including the most common 5^{12} , $5^{12}6^2$, and

5¹²6⁴ cages) that associate in different combinations to form structure I (sI) or structure II (sII) hydrates. The cage name base number indicates the 2-dimensional shape of the face, and the exponent indicates the number of sides. For example, a 5¹² cage has 12 pentagonal faces that combine to create a dodecahedron. Gas hydrates formed in industrial pipelines are generally of the sII form since natural gas contains larger molecules (e.g., propane) that are able to stabilize the larger cages of sII. The high pressure requirement to study natural gas or methane hydrates has led to the use of some analogs to study sII hydrates at lower pressures. This includes tetrahydrofuran (THF) hydrates [16,17] and cyclopentane (CyC5) hydrates. Recently, it has become more common to use CyC5 instead of THF as the hydrate former due to concerns of ice

Abbreviations: AAs, anti-agglomerants; CyC5, cyclopentane; DI, deionized; KHIs, kinetic hydrate inhibitors; LDHIs, low-dosage hydrate inhibitors; FGR, film growth rate; MD, molecular dynamic; MMF, micro-mechanical force; MO70T, mineral oil 70T; sI, structure I; sII, structure II; THF, tetrahydrofuran; THIs, thermodynamic hydrate inhibitors; WC, water content.

E-mail address: ckoh@mines.edu (C.A. Koh).

^{*} Corresponding author.

contamination and CyC5 hydrate having a larger subcooling range above the ice point [18]. For this reason, CyC5 hydrates were used for the experiments presented in this study.

An important interfacial parameter used to study hydrates is surface wettability, quantified through the contact angle. Having a high wettability (i.e., small contact angle) indicates that the hydrate surface is more water-wet and is more likely to promote hydrate agglomeration through capillary bridging, as described by Webb et al. [19]. The contact angle can be calculated using the Young equation [20], but since a hydrate surface does not meet the ideality requirements it cannot be calculated from interfacial and surface tensions. The contact angle on a hydrate surface must be measured directly. The contact angle and film growth behavior of water on CyC5 hydrates has been of interest because of their use as a low-pressure analog to gas hydrates. Differing results of contact angle have been reported by Brown et al. [21] and Thomas et al. [22]. These results were reconciled by Stoner et al. [23] who showed that the contact angle is highly dependent on the conditions of the hydrate surface (i.e., roughness and porosity), which can change with subcooling and annealing (conversion) time [24]. Stoner et al. also measured the film growth rate of cyclopentane hydrates, which showed a dependence on the magnitude of subcooling. The hydrate surfaces used by Brown et al.[21], Stoner et al.[23], and in this work are more representative of hydrate surfaces in pipelines, as they are not artificially leveled. Other studies have reported similar thermodynamic behavior for CyC5 [25], methane [26], and CO2 hydrates [27]. This interfacial behavior also can dictate hydrate agglomeration tendencies at a larger scale, making it very important to understand.

There are many different commercial additives that can be added to pipelines that will affect interfacial hydrate behavior in different ways. This includes: thermodynamic hydrate inhibitors (THIs) which shift the hydrate phase-boundary, and low-dosage hydrate inhibitors (LDHIs) [28,29], such as kinetic hydrate inhibitors (KHIs) which delay the onset of hydrate formation, or anti-agglomerants (AAs) that prevent extensive agglomeration allowing the system to flow as a hydrate slurry. THIs for hydrate mitigation can be challenging to use for full inhibition, however, as the amount of THI needed is on the order of 20-50 wt% or more of the water phase to be effective [28]. This can become quite costprohibitive for high water content (WC) systems. LDHIs, on the other hand, are needed in much smaller doses (<5 vol% of the oil phase [30]), but can be quite expensive, even for small quantities. AA performance (i. e., ability to prevent extensive hydrate agglomeration) has been suggested to be closely related to the compatibility of the AA structure with the oil phase [31].

There has also been observation of oils that do not form hydrates plugs, even when within the thermodynamic hydrate range. These oils have been termed "magic oils" or non-plugging oils. They display similar behavior to an oil system that has been dosed with a commercial AA. It is thought that the presence of natural surface active components in the oil (i.e., asphaltenes [32], resins [33]) critically affects interfacial behavior of hydrate bearing systems. A similar concept has been proposed by Høiland et al. [34] and Sjöblom et al. [35] who emphasized the importance of surface chemistry, emulsion stability, and shear on this behavior. Other studies have shown that emulsion stability alone may not be an indicator of an oil's non-plugging ability [36]. The effect of asphaltenes have been further studied for CO2 hydrate systems in a highpressure rheometer [37], CyC5 systems using an integrated thin film drainage apparatus to measure adhesive force [38], natural gas hydrates in a rocking cell [39], and CyC5 systems in a micro-mechanical force (MMF) apparatus [25] drawing similar conclusions to Sjöblom et al., where asphaltenes can decrease agglomeration and plugging [40]. However, it has also been suggested that asphaltenes may actually promote gas hydrate formation by acting as a nucleation site in a pipeline, both in experiment [41] and molecular dynamic (MD) simulations [42]. Further experiments have since highlighted the importance of the aggregation state of the asphaltenes present in the oil phase [43] and the presence of other components such as alcohols [44] in terms of the extent of agglomeration, which explains the varying effects of the asphaltene fraction.

In this paper, studies have been designed to understand the effects that the asphaltene fraction has on both the wettability behavior (contact angle) and film growth rate of CyC5 hydrates. It is suggested that the measurement of these properties, particularly contact angle, can act as an early indicator/first-pass test for determining the agglomeration/ plugging probability of an oil system, as shown in Fig. 1. Similar logic has been applied to other studies performed on commercial surfactants and their effects on cohesive force [45], where oils that reduce the cohesive force between hydrate particles correlate to oils that do not plug as easily [46]. Depending on the change in measured contact angle values with a natural surfactant (in an oil) present compared to a baseline CyC5 system with no presence of natural surfactant, an estimate $\,$ could be made of the need for further evaluation of the oil's behavior. Even though similar reasoning has been applied to other lab-scale apparatuses to test the potential non-plugging oil properties as described above, this technique is comparatively low-cost, easy to learn, and gives results quickly with ultra-low volumes of oil sample (micro-liters). It also removes the inherent risks of working with a high-pressure system, while maintaining the ability to work with a hydrate system directly. The studies presented here include measuring the contact angle and film growth rate of CyC5 hydrate systems dosed with different oils, different oil fractions, and un-treated oil at varying water contents to show the extent that asphaltenes could be responsible for altering the surface chemistry of the hydrate system. The results of this study have large implications on the techniques used to study the agglomeration behavior of oils and how a system under hydrate forming conditions can be

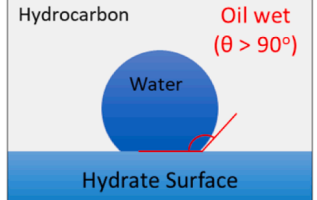
2. Methods and materials

2.1. Materials and apparatus

CyC5 (OmniSolve® CX2414-1, 99% purity) was used as a stable, low-pressure analog to sII natural gas hydrates. CyC5 hydrates form at mild conditions (atmospheric pressure, below 7.7 °C), making them relatively simple to create while also removing the safety concerns of using a high-pressure system. Spontaneous nucleation of CyC5 hydrates from liquid water can take days [48], so an ice seed is used to accelerate hydrate formation and growth consistent with other experiments [21]. The apparatus used here is the same as used by Stoner et al. [23] The oils and some of their relevant properties are summarized in Table S1.

2.2. Oil and water dosing technique

The technique used here has been slightly modified from Stoner et al. [23] to include preparation steps specific to adding a water phase and/ or an oil component to the hydrocarbon phase. For each experiment, the total volume of the mixture remains the same, but the overall volume of water and cyclopentane is changed to achieve the desired water content (0, 0.1, 0.25, 0.4 vol fraction). To dose the CyC5 with the desired oil, first a concentrated solution of 0.2 vol% oil in CyC5 is prepared, then diluted further with CyC5 to create a 0.02 vol% oil in CyC5 hydrocarbon phase. An ultra-low volume of 0.02 vol% oil is used to reduce visibility issues from the dark oils when viewing the samples under the microscope, and it allows for many repeated experiments using < 1 mL of oil. When performing experiments with both water and oil, the two phases are mixed for 10 min using a magnetic stirring plate to simulate the turbulence and phase mixing they would experience in a pipeline. Next, they are allowed to phase separate gravitationally for another 10 min to simulate a shut-in period. The water phase is extracted from the CyC5/ oil mixture and set aside. This water is used to form the ice particle and water droplet to create the hydrate particle as performed by Stoner et al. [23] In the case of 0 WC, deionized (DI) water is used to form the ice particle and water droplet. The contact angle is measured as shown by



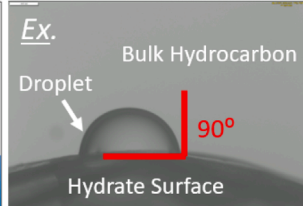


Fig. 1. Illustrations and an example of the qualitative information the value of the contact angle can give about its interaction with the oil phase, and ultimately its non-plugging potential. Here, contact angles less than 90° indicate a water-wet hydrate with a higher plugging potential, a contact angle of approximately 90° indicates neutral wetting ability, and a contact angle of greater than 90° indicates an oil-wet hydrate with a lower plugging potential, as shown by rocking cell results from Delgado-Linares et al. [47]. Modified from Bormashenko [20] and Stoner et al. [23].

Fig. 1, and the film growth rate is measured as described by Morrisey et al. [25] and Stoner et al. [23].

2.3. Oil fractionation

For some experiments, the oil was fractionated to isolate the effect of different fractions on the wettability and film growth. Asphaltenes were precipitated with n-heptane by using a heptane/oil ratio of 40 (ml/g) as described in Aguilera et al. [49]. The solids obtained here are the isolated asphaltene fraction, and the leftover liquid was evaporated under a vacuum to remove residual heptane to obtain the liquid de-asphalted oil. The isolated asphaltenes and binding resins were obtained using an oil separation scheme similar to that described by Graham et al. [50]. To create the model oils from the separated solid fractions (i.e. asphaltenes, asphaltenes + binding resins), the designated solids were added to toluene in a weight percentage reflective of their natural occurrence in the full crude oil. This toluene solution was then diluted in cyclopentane as described in the previous subsection. For the deasphalted fraction, the resulting liquid is used in place of the full crude for the same dilution.

Due to their varied nature, oils D, G, H, and O were chosen to cover a range of interfacial behavior and asphaltene content (low, intermediate, high) to understand how their polar fractions may change wettability and film growth.

3. Results and discussion

3.1. Addition of oil

As shown in Fig. 2, the addition of a non-plugging oil to CyC5 can change the wettability (i.e., the contact angle) of the hydrate surface. This could be attributed to the adsorption of the natural surfactant molecules (i.e., asphaltenes) at the interface [51]. These molecules can align to create a physical barrier between the hydrate surface and the water droplet, and since the surfactant molecules are hydrophobic, this makes it more difficult for the droplet to spread (Fig. 3) compared to the CyC5 baseline. This type of alignment has been shown with MD simulations [52] and is thought to be similar to the mechanism seen with commercial AAs [53,54]. The differences in contact angle behavior can

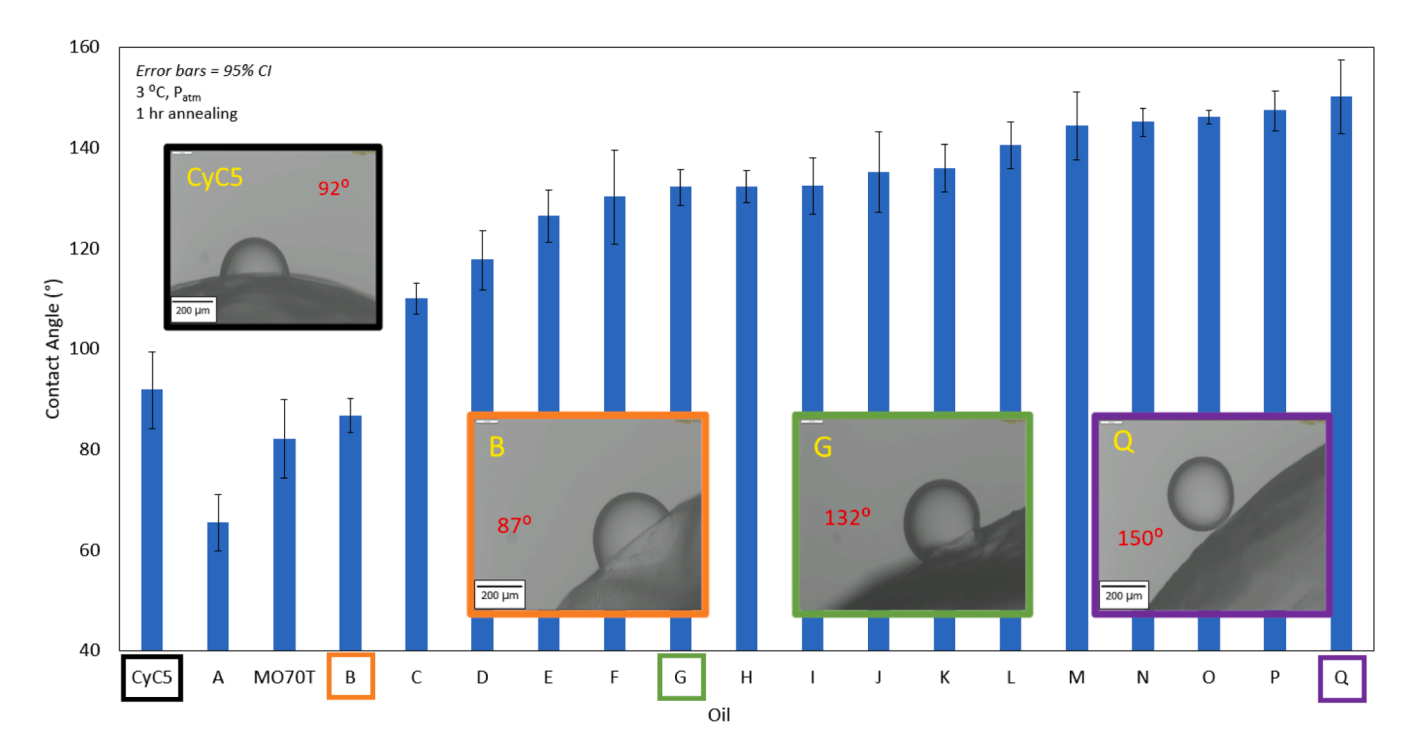
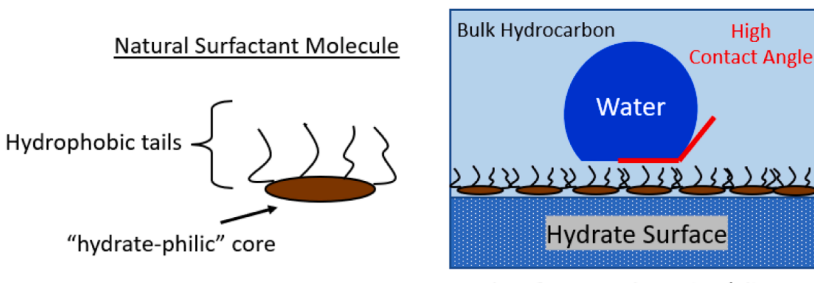
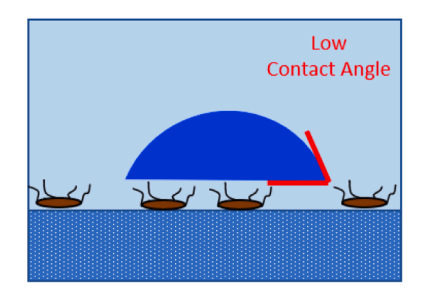


Fig. 2. Plot of contact angles of cyclopentane hydrate surfaces in the presence of different oils containing natural surfactants. Here, cyclopentane represents the baseline system with no presence of surfactants, MO70T is a commercially available model mineral oil, and each letter represents a different natural oil. Each bar represents the average contact angle measurements on a minimum of six DI water droplets and a minimum of three different hydrate particles (i.e., 12 angles). These experiments were performed at atmospheric pressure, a ΔT_{sub} of approximately 4°C, and an annealing time of 1 h. Error bars represent the 95% confidence interval. Images show examples of some contact angle measurements, labeled in red text. The images show examples of the baseline system (CyC5), a wetting oil (B), and two non-wetting oils (G, Q).





Good surfactant adsorption/alignment

Poor surfactant adsorption/alignment

Fig. 3. Illustration of how natural surfactant molecules align at the interface and how it may affect the spreading of water over a hydrate surface. Modified from Hu [31].

be attributed to the polar content (typically the asphaltene fraction [55]) of each oil. A visual representation of example contact angles can be seen in Fig. 2. It should be noted that the droplets in the images appear to be on an incline. However, the images are taken from the top view of the hydrate particle and the droplets are on a horizontal surface. The baseline CyC5 value for contact angle and FGR are in line with the value published by Brown et al. [21], Stoner et al. [23], and Morrisey et al. [25]. The model oil Mineral Oil 70 T is represented by the abbreviation MO70T.

As shown in Fig. 4a, oils that did not have a large effect on the contact angle, also did not have an effect on the Film Growth Rate (FGR). This can be attributed to two potential phenomena, the first being that more spreading of the droplet results in more points of contact where seeding of the hydrate film can occur on the surface to induce film nucleation. Second, if the surface active components are aligning poorly and/or sparsely at the interfaces, there are little to no mass transfer limitations or kinetic inhibition mechanisms affecting the film growth, and it proceeds in the same way as the baseline system. For some oils with higher contact angles, the FGR was decreased (Fig. 4(a)). The more non-wetting oils have a larger presence of surface active components), which can align at the interface, causing both a higher contact angle and in some cases lower rates of film growth (Fig. 4(a)). Hence, the potential relationship between the natural AAs in an oil and natural KHI potential based on contact angle and film growth values is oil dependent. There is a potential relationship between contact angle and asphaltene content of the oils, where higher amounts of asphaltenes tend to have higher

contact angles that approach 180° (Fig. 4b).

The relationship between asphaltene content, contact angle, and FGR indicates that some oils not only display interfacial characteristics similar to commercial AA additives (through contact angle), but can also delay the growth of hydrate films similar to KHIs. Similar behavior has been noted for methane hydrate formation in MD simulations [56] and in experiment with commercial AAs [57]. As changes in contact angle behavior are observed at such small concentrations (0.02 vol% oil in CyC5), a complementary study was also performed to see if this behavior is exaggerated at higher concentrations of oil for 6 oils.

3.2. Varying concentration of oil

For this set of experiments, higher concentrations of oil were tested to determine the effect of adding more surface active components to the system. Ultra-low oil concentrations are used in part due to the affect oils have on visibility. As many of the oils are very dark, higher concentrations give significantly decreased or completely non-visible hydrate particles. For the darker oils (O, D, and C), the contact angles and film growth were measured at additional concentrations of 0.2 and 2 vol %. For the lighter oils with less visibility limitations (MO70T, A, and B), contact angles and film growth were measured at concentrations of up to 5 vol%. Oil O approaches complete de-wetting (contact angle of 180°) at 0.2 vol%, so contact angle and film growth behavior was measured at intermediate volumes (0.04, 0.08, and 0.16 vol%). A summary of the wettability and film growth results as a function of oil concentration can

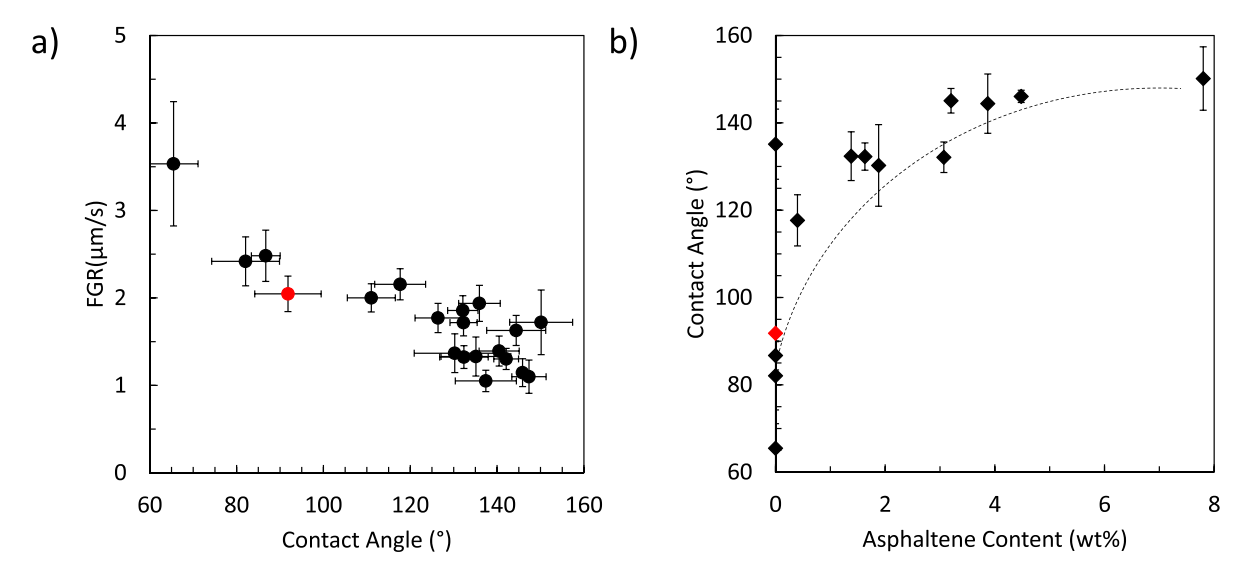


Fig. 4. (a) Plot of contact angle vs. film growth rates (b) Plot of contact angle vs. asphaltene content of the oil. The error bars for both plots (horizontal and vertical) represent 95% confidence intervals from a minimum of 6 water droplets on 3 or more hydrate particles. The dotted line is only to guide the eye. The red points on both graphs represent the cyclopentane baseline system.

be seen in Fig. 5 a and b, respectively. A list of the contact angle values can be seen in Table S2. For all oils tested, increasing the concentration of oil in CyC5 resulted in a higher contact angle. The lighter oils start out with significantly lower contact angles ($<100^{\circ}$) than the darker oils (greater than 110°), but the addition of more oil did increase the contact angle. The darker oils had a more drastic increase, where the value of their contact angles approached 180° by 2 vol%. This behavior is attributed to a larger concentration of surface active components that are aligning and adsorbing at the interface resulting in less spreading of the droplet.

Increasing the concentration of oil affected the film growth in a similar way to contact angle, where addition of more oil resulted in a slower film growth rate. For all oils tested, the FGR was reduced when the amount of oil in the system was increased, as shown in Fig. 5b. Again, this can be attributed to an increase in surface active components that act as a mass transfer barrier, as well as lower areas of contact to seed hydrate film growth over the surface of the droplet. A visual representation of an example oil at varying concentrations can be seen in Fig. 5c.

3.3. Addition of oil and water

To simulate an environment more similar to the field, a water phase was added as described in the methods section. Four water contents (0, 0.1, 0.25, 0.4 in volume fraction) were tested. In larger scale rocking cell tests, oils typically fail between 0.3 and 0.4 WC, which dictated the upper limit of water contents tested [58]. For the two potential nonplugging oils tested (O and K), the contact angle was decreased as more water was added. For potential plugging oil C, the addition of water did not affect the contact angle, indicating the poor performance

of any surface active components in the oil phase. This data is shown in Fig. 6a. A list of the contact angle values can be seen in Table S3. Here, not only are the surface active components being diluted with the addition of more water (overall volume stays the same between water contents), but small amounts of water that may be trapped in the oil phase after mixing may be aligning at the interface. This would increase the height of the quasi-liquid layer [59] and result in further spreading of the water droplet on the hydrate surface. Trends in the FGR from varying WCs were not seen, the data is present in figure S1. Visual representation of selected oils at varying WCs can be seen in Fig. 6b.

3.4. Effect of different oil fractions

Typically, changes in wettability/morphology and nucleation/ agglomeration behavior of a hydrate system are thought to be affected by the asphaltene phase [60,61], but can be also affected by other fractions, including resins [62,63] and waxes [64,65]. To separate the effect from different fractions, both contact angle and film growth were measured for different portions of the oils. This includes the full oil, isolated asphaltene and binding resin fractions dissolved in toluene, isolated asphaltene fraction dissolved in toluene, and the deasphalted portion of oil. It is assumed that the full crude oil has the most surface active components followed by the combined asphaltene and resin fractions, the asphaltene fraction, and then the deasphalted oil. Removal of certain fractions can alter the behavior of the interfacial behavior of the oil [66].

For oil O, the removal of more surface active components resulted in a steady decline in the contact angle and an increase in the FGR approaching the baseline. Oil O has a very high contact angle which indicates that its surface active components adsorb and align well at the

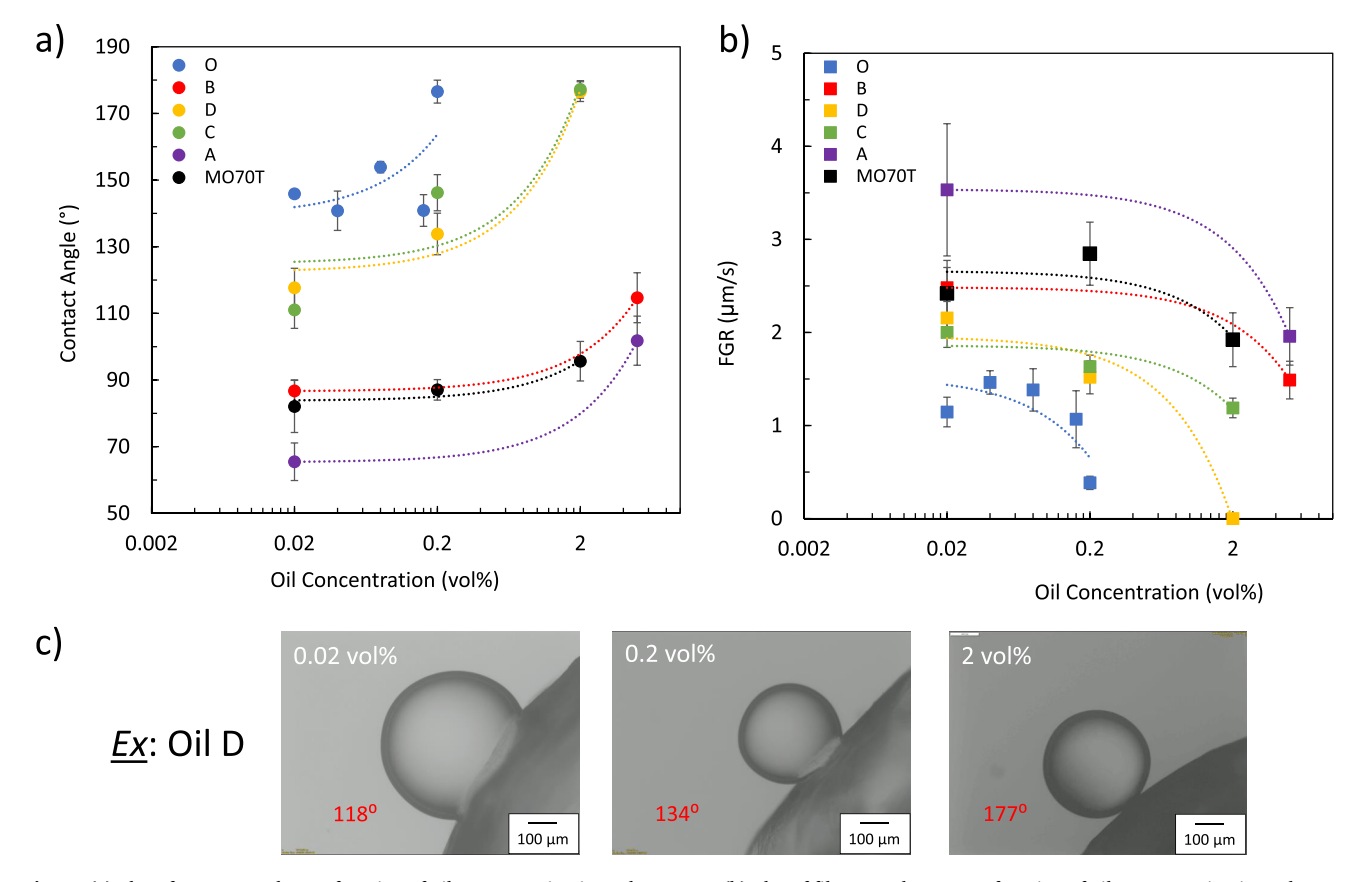


Fig. 5. (a) Plot of contact angle as a function of oil concentration in cyclopentane. (b) Plot of film growth rate as a function of oil concentration in cyclopentane. For each plot, every point represents the average contact angle measurements on a minimum of six DI water droplets and a minimum of three different hydrate particles (i.e., 12 angles). These experiments were performed at atmospheric pressure, a ΔT_{sub} of approximately 4°C, and an annealing time of 1 h. Error bars represent the 95% confidence interval. Dotted lines are to guide the eye. (c) Examples of contact angle images at varying concentrations of oil. The images show examples of oil D.

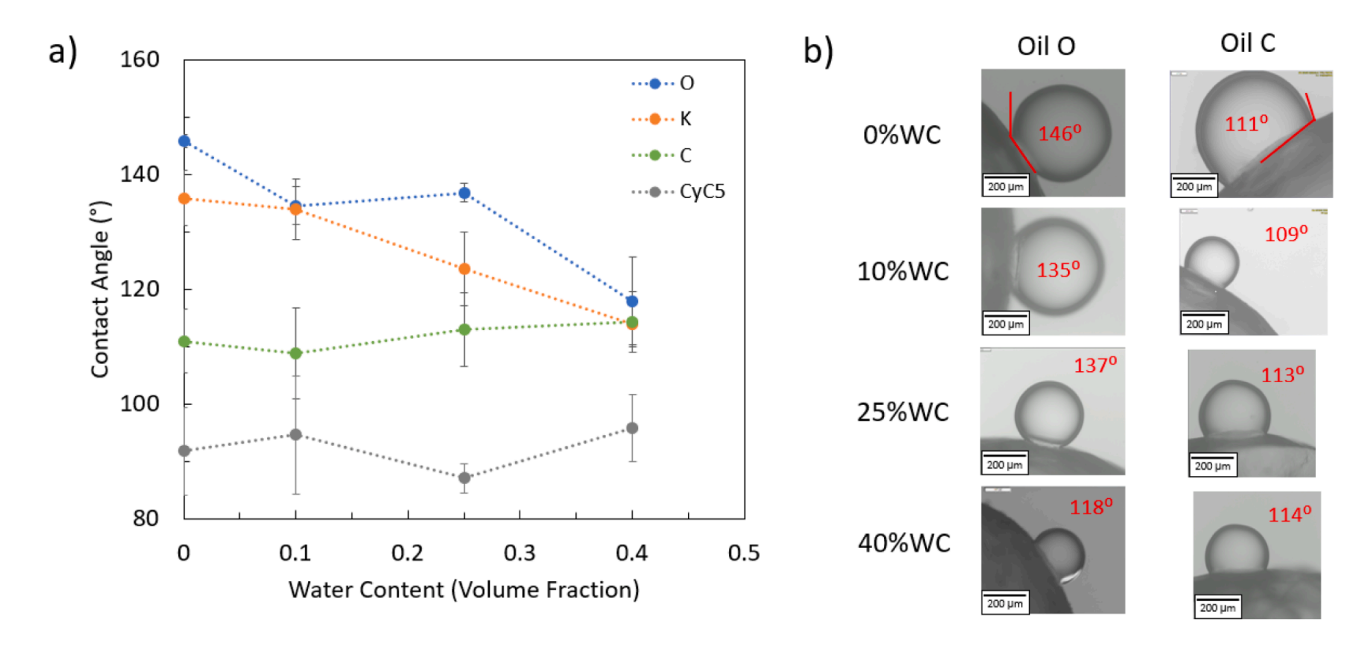


Fig. 6. (a) Plot of contact angle vs. water content. Here, each point represents the average contact angle measurements on a minimum of six DI water droplets and a minimum of three different hydrate particles (i.e., 12 angles). These experiments were performed at atmospheric pressure, a ΔT_{sub} of approximately 4°C, and an annealing time of 1 h. Error bars represent the 95% confidence interval. Dotted lines are to guide the eye. (b) Examples of contact angle images at varying water volume fractions. The images show examples of oils O and C.

interface which changes both wettability and film growth behavior. For oil H, both the contact angle and FGR stay approximately the same when more oil fractions are removed. This indicates that the surface active components in the asphaltene and resin phases are not contributing as much to its wettability and film growth behavior. For oils G and D, the behavior of the isolated asphaltene/resin fractions and the isolated asphaltene fraction is not in line with the full oil and deasphalted oil, which have approximately the same contact angles and similar FGRs.

This is attributed to the addition of toluene, as isolated asphaltenes and resins are solids. The addition of toluene has been shown to change the aggregation state of the oil [67,68], which will change its interfacial behavior. A summary of the contact angle results and FGR results can be seen in Fig. 7a and 7b, respectively. Images of the contact angle of a select oil can be seen in Fig. 7c.

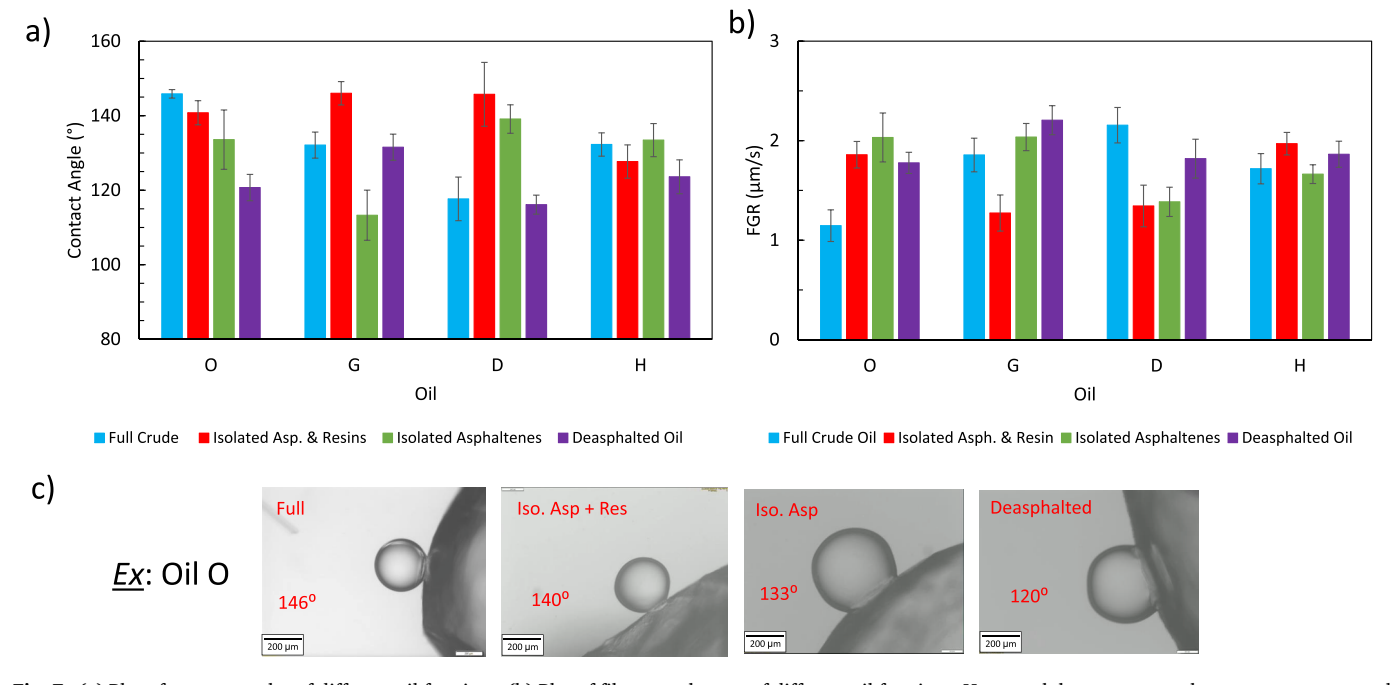


Fig. 7. (a) Plot of contact angles of different oil fractions. (b) Plot of film growth rates of different oil fractions. Here, each bar represents the average contact angle measurements on a minimum of six DI water droplets and a minimum of three different hydrate particles (i.e., 12 angles). The experiments in plots a and b were performed at atmospheric pressure, a ΔT_{sub} of approximately 4°C, and an annealing time of 1 h. Error bars represent the 95% confidence interval. (c) Examples of contact angle images for each crude oil fraction. The images show examples of oil O.

3.5. Effect of film growth on droplet morphology

Stoner et al. [23] introduced the concept of the crystallization angle. The crystallization angle is the angle at the original three-phase line after film growth has occurred, and it may be different than the contact angle. Here, the initial film growth that propagates from the three phase line (hydrate, water droplet, bulk oil) can change this angle, as the film is weak and pliable. They showed that in pure cyclopentane systems, the crystallization angle was higher than the contact angle, regardless of annealing time or subcooling. Here, the addition of oil slightly decreases or does not change the crystallization angle compared to the contact angle for most oils, as shown in Figure S2. This is attributed to the alignment of surface active components at the interface that discourage spreading of the water droplet, as shown by the difference in contact angles of CyC5 with oil compared to CyC5 without oil. Although the angle may be altered over time with film growth or capillary suction that changes the shape of the droplet, the final crystallization angle is still similar to the contact angle. However, for CyC5, MO70T, and oil B, the crystallization angle is higher than the contact angle. This is due to the capillary suction pulling the water into the hydrate. The inward force felt by the film is strong enough to bend the film toward the surface before it completely covers the droplet and stabilizes the shape which results in a higher angle (see Stoner et al., Fig. 9).

Stoner et al. also noted a dimpling effect on some of the film covered water droplet. The final shape of the film covered droplet would have a concave center. Here, the capillary suction of the water into the porous

hydrate surface was fast enough compared to the film growth that the film eventually folded in on itself, resulting in the dimple. Dimpling was not always present with different oils. In this work, three morphology change scenarios were observed.

The first scenario is when film growth and capillary suction start at approximately the same time, or suction begins before film growth. Here, the droplet height steadily decreases until film growth is complete. The capillary suction pushes the film outward (as described in the previous paragraph) which changes the shape of the film covered droplet. The final shape does not resemble the initial water droplet. This results in a very slightly convex shape across the top of the shell, a shell with a flat top, or a dimpled shell as described by Stoner et al. This scenario is shown in Fig. 8a.

The second is when film growth begins before capillary suction is observed. The height of the droplet stays consistent (only moving slightly up or down) until suction starts, while the film maintains the shape of the original droplet. Next, the droplet height decreases sharply as capillary suction begins. This results in the bottom half of the remaining hydrate shell appearing to look about the same shape as the initial droplet, and the top half losing its initial shape as the height of the droplet decreases. As film growth completes, the bottom half maintains its shape compared to the initial droplet. The top half appears flat or dimpled. This scenario is shown in Fig. 8b.

The third scenario is when there is no capillary suction and only film growth. Here, the droplet height steadily increases as it is pushed upward by film growth. The film will maintain its initial shape. The growth

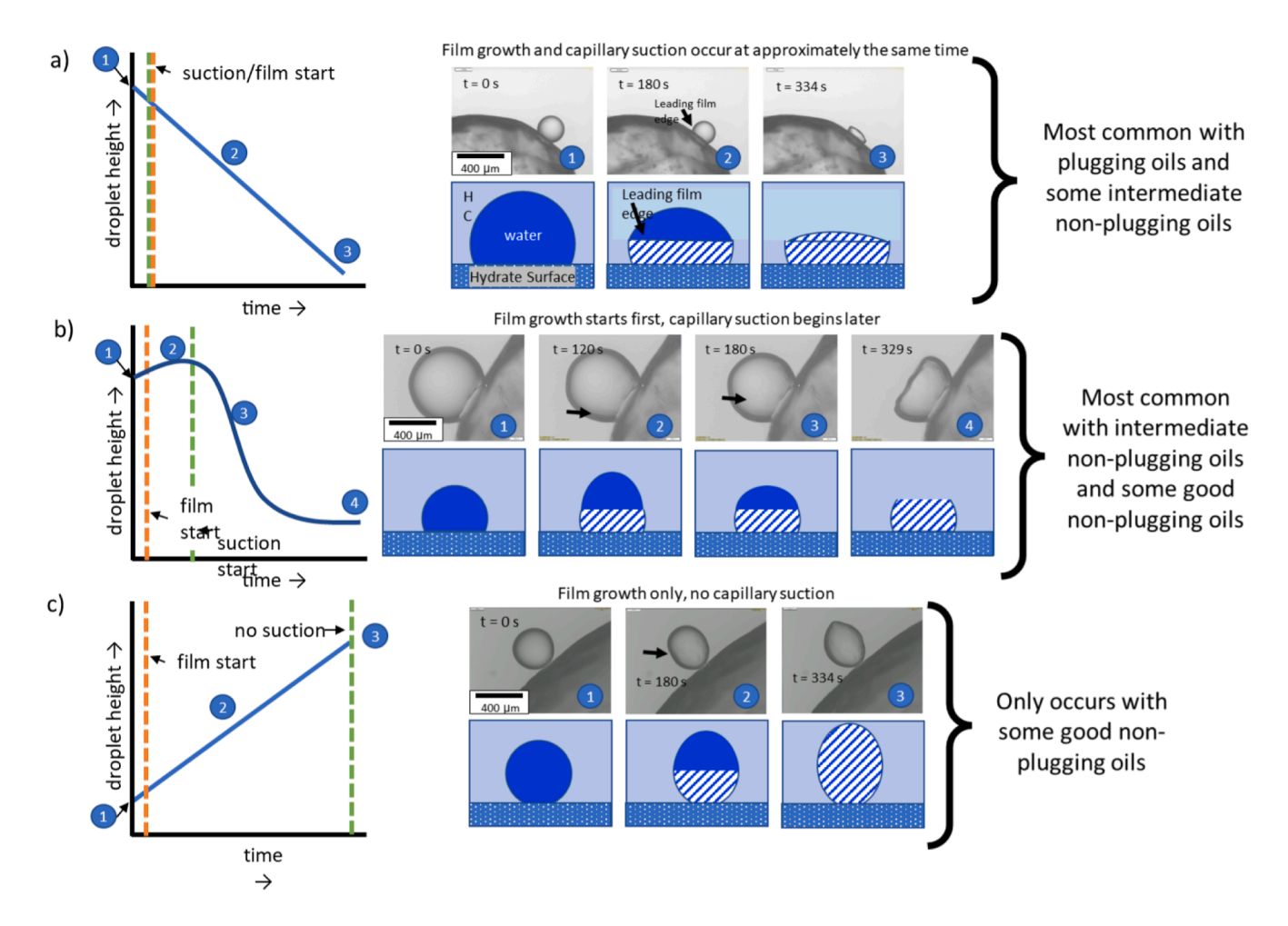


Fig. 8. Typical droplet height profiles over time along with film growth visuals and mechanistic diagrams of different scenarios regarding hydrate film growth and capillary suction. (a) approximate simultaneous start of film growth and capillary suction, or capillary suction occurs before film growth (b) film growth occurs before capillary suction; (c) no capillary suction, film growth only.

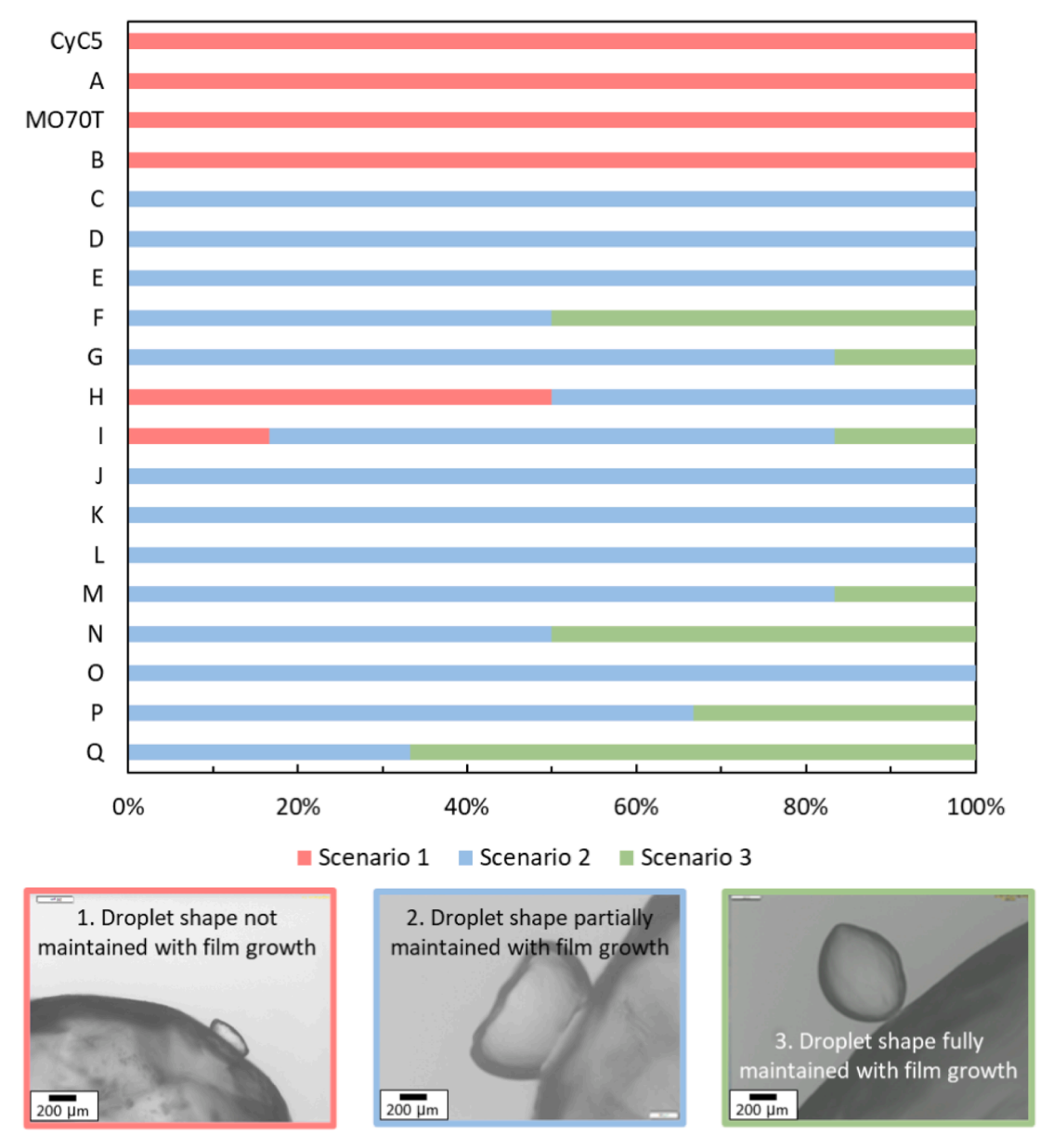


Fig. 9. Top: Breakdown of the percentage of each morphology change scenario seen for each oil. Bottom: Illustration of each scenario, as explained in detail by Fig. 8.

of the film slowly pushes the remaining water droplet upward until film growth completes and no dimpling occurs. The final shell appears more ellipsoidal than the original spherical droplet. This scenario is shown in Fig. 8c. Scenarios one and two are the most common and were seen regardless of the type of oil. Scenario three was less common and was only observed for some trials with oils that had very high contact angles.

Each oil showed one or more of these scenarios during the contact angle experiments. The breakdown of the scenarios seen for each oil is shown in Fig. 9. Oils CyC5, MO70T, A, and B only displayed scenario 1, and also had the lowest contact angles of all oils tested. Scenario 2 was the most common, and scenario 3 was the least common. The changes in droplet morphology can give information on the competing effects of capillary suction of water into the hydrate vs. the film growth rate. Although the oils with the higher wettability (i.e., lowest contact angle) are considered more at risk for plugging, they may also be removing free water from the bulk which can affect their bedding and deposition behavior [69].

4. Conclusions

Multiple sets of experiments were performed to examine wettability behavior (quantified using the contact angle) and film growth of cyclopentane hydrates in the presence of oil, varying oil concentrations, varying water contents, and varying isolated fractions of crude oil. The addition of oil showed a relationship between low wettability and slower film growth rates compared to the baseline system which was attributed to asphaltene content and better adsorption/alignment of natural surfactants at the hydrate interface. The natural surfactant alignment is thought to reduce points of contact for nucleation and can also act as a mass transfer barrier to slow the film growth over the droplet. Here, oil samples contained asphaltene fractions that mostly were between 0 and 4.5 wt%. It would be interesting in the future to test oils with higher asphaltene contents to extend such analyses.

The next set of experiments looked at the effects of varying oil concentration on the wettability and film growth. As the concentration of oil added was increased, the wettability and FGR both decreased. The decrease was more drastic for the potential non-plugging oils and was

attributed to better alignment/adsorption at the hydrate interface. When water content was varied for a select set of oils, the wettability increased with increasing water contents while FGR remained relatively unchanged. The increase in wettability is attributed to an overall decrease in concentration of natural surfactants as the water content increases.

When different oil fractions were isolated and tested, it showed how certain fractions are responsible for the change in wettability and film growth behavior of hydrate surfaces. For the better performing non-plugging oil (O), the more surface active components that were removed (i.e., full crude, asphaltene + resins, asphaltenes, deasphalted) the higher the wettability and higher the FGR. For one of the intermediate performing non-plugging oils (H), the surface activity seemed to stay approximately the same when different fractions were isolated, which resulted in little to no change in wettability and FGR. For the other intermediate performing non-plugging oils (D and G), the addition of toluene to the isolated oil fractions changed the aggregation state of the surface active components, which results in a lower wettability and a slower film growth rate than the full crude oil.

A conceptual picture of the transient change in droplet shape/height during hydrate film growth and capillary suction was also proposed. Depending on the order of the start of film growth or capillary suction, the film covered droplets are eventually either flat/dimpled and do not (or only partially) resemble their initial droplet shape, or they become more ellipsoidal with no dimple and mostly maintain their initial droplet shape. Droplets that do not maintain or partially maintain their shape are typically plugging to intermediate non-plugging oils (based on wettability) and droplets that maintain their shape are typically good non-plugging oils with very low wettability).

The results described here highlight the vast amount of information of wetting ability and film growth that can be obtained from measuring the contact angle. Each of these observed interfacial behaviors gives information on larger scale phenomena including hydrate agglomeration, and could be used as a tool to estimate the plugging probability of an oil using a very small sample volume.

CRediT authorship contribution statement

Hannah M. Stoner: . Jefferson Moak: . Jose G. Delgado-Linares: Writing – review & editing, Supervision, Methodology, Conceptualization. Carolyn A. Koh: Writing – review & editing, Resources, Supervision, Investigation, Funding acquisition, Conceptualization.

Declaration of Competing Interest

The authors declare that they have no known competing financial interests or personal relationships that could have appeared to influence the work reported in this paper.

Data availability

Data will be made available on request.

Acknowledgement

The authors would like to thank the NSF CBET Award #2015201 (H. M.S. and C.A.K.) for funding. Thanks to the Center for Hydrate Research for the facilities used and oils provided for this study. Thanks also extended to Dr. Jon Wells and Chaffin Ross for their help in refining the technique used to measure the contact angles in this study, and to Erik Siekkinen, Makenna Phillips, and Julia Cacciavillani for their contributions of IFT measurements.

Appendix A. Supplementary material

Supplementary data to this article can be found online at https://doi.

org/10.1016/j.fuel.2023.129422.

Reference

- Sir Humphry Davy. On a Combination of Oxymuriatic Gas and Oxygene Gas. R Soc Publ 1811;101:155–62.
- [2] Makogon Y. Features of natural gas fields exploitation in permafrost zone. Gazov Promyshlennost 1966;9:1–17.
- [3] Collett T, Lewis K, Zyrianova M, Haines S, Schenk C, Mercier T, et al. Assessment of undiscovered gas hydrate resources in the north slope of alaska, 2018. USGS 2019: 2016–9. https://doi.org/10.3133.
- [4] Thomas C, Mousis O, Picaud S, Ballenegger V. Variability of the methane trapping in martian subsurface clathrate hydrates. Planet Space Sci 2009;57:42–7. https:// doi.org/10.1016/j.pss.2008.10.003.
- [5] Miller SL. the occurrence of gas hydrates in the solar system. Proc Natl Acad Sci 1961;47:1798–808. https://doi.org/10.1073/pnas.47.11.1798.
- [6] Kamata S, Nimmo F, Sekine Y, Kuramoto K, Noguchi N, Kimura J, et al. Pluto's ocean is capped and insulated by gas hydrates. Nat Geosci 2019;12:407–10. https://doi.org/10.1038/s41561-019-0369-8.
- [7] Ho-Van S, Bouillot B, Douzet J, Babakhani SM, Herri JM. Cyclopentane hydrates-A candidate for desalination? J Environ Chem Eng 2019;7:103359. https://doi.org/ 10.1016/j.jece.2019.103359.
- [8] Montazeri SM, Kolliopoulos G. Hydrate based desalination for sustainable water treatment: a review. Desalination 2022;537:115855. https://doi.org/10.1016/j. desal 2022 115855
- [9] Wang S, Hu S, Brown EP, Nakatsuka MA, Zhao J, Yang M, et al. High pressure micromechanical force measurements of the effects of surface corrosion and salinity on CH4/C2H6 hydrate particle-surface interactions. Phys Chem Chem Phys 2017;19:13307–15. https://doi.org/10.1039/c7cp01584d.
- [10] Misyura S, Strizhak P, Meleshkin A, Morozov V, Gaidukova O, Shlegel N, et al. A review of gas capture and liquid separation technologies by CO2 gas hydrate. Energies 2023;16:1–20. https://doi.org/10.3390/en16083318.
- [11] Zhu Y, Wang P, Pang S, Zhang S, Xiao R. A review of the resource and test production of natural gas hydrates in china. Energy Fuel 2021;35:9137–50. https://doi.org/10.1021/acs.energyfuels.1c00485.
- [12] Kezirian MT, Phoenix SL. Natural gas hydrate as a storage mechanism for safe, sustainable and economical production from offshore petroleum reserves. Energies 2017:10. https://doi.org/10.3390/en10060828.
- [13] He Y, Sun M-T, Chen C, Zhang G, Chao K, Lin Y, et al. Surfactant-based promotion to gas hydrate formation for energy storage. J Mater Chem A 2019. https://doi. org/10.1039/c9ta07071k.
- [14] Mimachi H, Takahashi M, Takeya S, Gotoh Y, Yoneyama A, Hyodo K, et al. Effect of long-term storage and thermal history on the gas content of natural gas hydrate pellets under ambient pressure. Energy Fuel 2015;29:4827–34. https://doi.org/ 10.1021/acs-energyfuels.5bi00832
- [15] Hammerschmidt EG. Formation of gas hydrates in natural gas transmission lines. Ind Eng Chem 1934;26:851–5. https://doi.org/10.1021/ie50296a010.
- [16] Devarakonda S, Groysman A, Myerson AS. THF-water hydrate crystallization: an experimental investigation. J Cryst Growth 1999;204:525–38. https://doi.org/ 10.1016/S0022-0248(99)00220-1.
- [17] Li W, Pang J, Peng L, Fang B, Ou W, Tao Z, et al. microscopic insights into the effects of anti-agglomerant surfactants on surface characteristics of tetrahydrofuran hydrate. Energy Fuel 2023;37:3741–51. https://doi.org/10.1021/ acs.energyfuels.2c04254.
- [18] Taylor CJ, Dieker LE, Miller KT, Koh CA, Sloan ED. Micromechanical adhesion force measurements between tetrahydrofuran hydrate particles. J Colloid Interface Sci 2007;306:255–61. https://doi.org/10.1016/j.jcis.2006.10.078.
- [19] Webb EB, Koh CA, Liberatore MW. High pressure rheology of hydrate slurries formed from water-in- mineral oil emulsions. Ind Eng Chem 2014:6998–7007.
- [20] Bormashenko EY. 2 Wetting of surfaces: the contact angle. Phys. Wetting Phenom. Appl. fluids surfaces. 1st ed., Berlin: de Gruyter; 2017, p. 20–39.
- [21] Brown EP, Hu S, Wells J, Wang X, Koh CA. Direct measurements of contact angles on cyclopentane hydrates. Energy Fuel 2018;32:6619–26. https://doi.org/ 10.1021/acs.energyfuels.8b00803.
- [22] Thomas F, Dalmazzone D, Morris JF. Contact angle measurements on cyclopentane hydrates. Chem Eng Sci 2021;229:116022. https://doi.org/10.1016/j. ces.2020.116022.
- [23] Stoner HM, Phan A, Striolo A, Koh CA. Water wettability coupled with film growth on realistic cyclopentane hydrate surfaces. Langmuir 2021:12447–56. https://doi. org/10.1021/acs.langmuir.1c02136.
- [24] Servio P, Englezos P. Morphology of methane and carbon dioxide hydrates formed from water droplets. AIChE J 2003;49:269–76. https://doi.org/10.1002/ aic.690490125.
- [25] Morrissy SA, McKenzie AJ, Graham BF, Johns ML, May EF, Aman ZM. Reduction of clathrate hydrate film growth rate by naturally occurring surface active components. Energy Fuel 2017;31:5798–805. https://doi.org/10.1021/acs. apprentials.6302042
- [26] Freer EM, Sami Selim M, Dendy SE. Methane hydrate film growth kinetics. Fluid Phase Equilib 2001;185:65–75. https://doi.org/10.1016/S0378-3812(01)00457-5.
- [27] Uchida T, Ikeda IY, Takeya S, Ebinuma T, Nagao J, Narita H. CO2 hydrate film formation at the boundary between CO2 and water: effects of temperature, pressure and additives on the formation rate. J Cryst Growth 2002;237–239:383–7. https://doi.org/10.1016/S0022-0248(01)01822-X.
- [28] Kelland MA. History of the development of low dosage hydrate inhibitors. Energy Fuel 2006;20:825–47. https://doi.org/10.1021/ef050427x.

- [29] Perrin A, Musa OM, Steed JW. The chemistry of low dosage clathrate hydrate inhibitors. Chem Soc Rev 2013;42:1996–2015. https://doi.org/10.1039/ c?ps35340g
- [30] Creek JL. Efficient hydrate plug prevention. Energy Fuel 2012;26:4112–6. https://doi.org/10.1021/ef300280e.
- [31] Hu S. Interfacial Properties of CH4/C2H6 Gas Hydrate Particles with Chemical Additives. Colorado School of Mines, 2019.
- [32] Zhang D, Creek J, Marshall AG, Rodgers RP, Mullins OC. Asphaltenes problematic but rich in potential. Oilf Rev 2007.
- [33] Stoporev AS, Semenov AP, Medvedev VI, Mendgaziev RI, Istomin VA, Sergeeva DV, et al. Formation and agglomeration of gas hydrates in gas organic liquid water systems in a stirred reactor: role of resins/asphaltenes/surfactants. J Pet Sci Eng 2019;176:952–61. https://doi.org/10.1016/j.petrol.2019.02.002.
- [34] Høiland S, Askvik KM, Fotland P, Alagic E, Barth T, Fadnes F. Wettability of Freon hydrates in crude oil/brine emulsions. J Colloid Interface Sci 2005;287:217–25. https://doi.org/10.1016/j.jcis.2005.01.080.
- [35] Sjöblom J, Øvrevoll B, Jentoft GH, Lesaint C, Palermo T, Sinquin A, et al. Investigation of the hydrate plugging and non-plugging properties of oils. J Dispers Sci Technol 2010;31:1100–19. https://doi.org/10.1080/01932690903224698.
- [36] Aman ZM, Syddall WGT, Haber A, Qin Y, Graham B, May EF, et al. Characterization of crude oils that naturally resist hydrate plug formation. Energy Fuel 2017;31:5806–16. https://doi.org/10.1021/acs.energyfuels.6b02943.
- [37] Sandoval GAB, Thompson RL, Sad CMS, Teixeira A, Soares EJ. Influence of adding asphaltenes and gas condensate on CO 2 hydrate formation in water–CO 2 –oil systems. Energy Fuel 2019;33:7138–46. https://doi.org/10.1021/acs. energyfuels.9b01222.
- [38] Chen Z, Liu B, Manica R, Liu Q, Xu Z. Interaction between the cyclopentane hydrate particle and water droplet in hydrocarbon oil. Langmuir 2020;36:2063–70. https://doi.org/10.1021/acs.langmuir.9b03887.
- [39] Daraboina N, Pachitsas S, Von Solms N. Natural gas hydrate formation and inhibition in gas/crude oil/aqueous systems. Fuel 2015;148:186–90. https://doi. org/10.1016/j.fuel.2015.01.103.
- [40] Fadnes FH. Natural hydrate inhibiting components in crude oils. Fluid Phase Equilib 1996;117:186–92. https://doi.org/10.1016/0378-3812(95)02952-4.
- [41] Leporcher EM, Peytavy JL, Mollier Y, Sjoblom J, Labes-Carrier C. Multiphase Transportation: hydrate plugging prevention through crude oil natural surfactants. Soc. Pet. Eng., New Orleans, LA: 1998, p. 509–24. https://doi.org/10.2118/49172-MS.
- [42] Zi M, Chen D, Ji H, Wu G. Effects of Asphaltenes on the formation and decomposition of methane hydrate: a molecular dynamics study. Energy Fuel 2016;30:5643–50. https://doi.org/10.1021/acs.energyfuels.6b01040.
- [43] Gao S. Investigation of interactions between gas hydrates and several other flow assurance elements. Energy Fuel 2008;22:3150–3. https://doi.org/10.1021/ ef800189k.
- [44] Delgado-linares JG, Salmin DC, Stoner H, Wu DT, Zerpa LE, Koh CA. Effect of Alcohols on Asphaltene-Particle Size and Hydrate Non-Plugging Behavior of Crude Oils. Offshore Technol. Conf., Houston. TX: 2020.
- [45] Brown EP, Koh CA. Micromechanical measurements of the effect of surfactants on cyclopentane hydrate shell properties. Phys Chem Chem Phys 2016;18:594–600. https://doi.org/10.1039/c5cp06071k.
- [46] McKenzie AJ, Rasheed MD, Morrissy SA, Norris BWE, Johns ML, May EF, et al. Exploiting natural oil surfactants to control hydrate aggregation. Energy Fuel 2022; 36:9982–9. https://doi.org/10.1021/acs.energyfuels.2c01417.
- [47] Delgado-Linares JG, Pickarts MA, Zerpa LE, Koh CA. Outlook on the role of natural surfactants on emulsion stability and gas hydrate antiagglomeration in crude oil systems. Energy Fuel 2022;36:10732–50. https://doi.org/10.1021/acs. energyfiele 2021064
- [48] Larsen R, Lund A, Andersson V, Hjarbo KW. Conversion of water to hydrate particles. Proc - SPE Annu Tech Conf Exhib 2001:1905–9. https://doi.org/ 10.2523/71550-ms.
- [49] Aguilera BM, Delgado JG, Cárdenas AL. Water-in-oil emulsions stabilized by asphaltenes obtained from venezuelan crude oils. J Dispers Sci Technol 2010;31: 359–63. https://doi.org/10.1080/01932690903196144.

- [50] Graham BF, May EF, Trengove RD. Emulsion inhibiting components in crude oils. Energy Fuel 2008;22:1093–9. https://doi.org/10.1021/ef700529m.
- [51] Langevin D, Argillier JF. Interfacial behavior of asphaltenes. Adv Colloid Interface Sci 2016;233:83–93. https://doi.org/10.1016/j.cis.2015.10.005.
- [52] Mikami Y, Liang Y, Matsuoka T, Boek ES. Molecular dynamics simulations of asphaltenes at the oil-water interface: from nanoaggregation to thin-film formation. Energy Fuel 2013;27:1838–45. https://doi.org/10.1021/ef301610q.
- [53] Naullage PM, Bertolazzo AA, Molinero V. How do surfactants control the agglomeration of clathrate hydrates? ACS Cent Sci 2019;5:428–39. https://doi. org/10.1021/acscentsci.8b00755.
- [54] Bui T, Phan A, Monteiro D, Lan Q, Ceglio M, Acosta E, et al. Evidence of structureperformance relation for surfactants used as antiagglomerants for hydrate management. Langmuir 2017;33:2263–74. https://doi.org/10.1021/acs. langmuir.6b04334.
- [55] Buckley JS, Liu Y, Xie X, Morrow NR. Asphaltenes and crude oil wetting The effect of oil composition. SPE J 1997;2:107–19. https://doi.org/10.2118/35366-PA.
- [56] Zi M, Chen D, Wu G. Molecular dynamics simulation of methane hydrate formation on metal surface with oil. Chem Eng Sci 2018;191:253–61. https://doi.org/ 10.1016/j.ces.2018.06.070.
- [57] Ning F, Guo D, Ud S, Zhang H, Ou W, Fang B, et al. The kinetic effects of hydrate anti-agglomerants / surfactants. Fuel 2022;318:123566. https://doi.org/10.1016/ j.fuel.2022.123566.
- [58] Delgado-Linares JG, Majid AAA, Zerpa LE, Koh CA. Reducing THI injection and gas hydrate agglomeration by under-inhibition of crude oil systems. Proc Annu Offshore Technol Conf 2021. https://doi.org/10.4043/31161-MS.
- [59] DZYALOSHINSKII IE, LIFSHITZ EM, PITAEVSKII LP, Priestley MG. The general theory of van der Waals forces. Pergamon Press plc; 1992. 10.1016/b978-0-08-036364-6.50039-9.
- [60] Zhang J, Li C, Yang F, Shi L, Yao B, Sun G. Influences of asphaltene subfractions with different polarities on hydrate growth at water/oil interface. Fuel 2022;330: 125546. https://doi.org/10.1016/j.fuel.2022.125546.
- [61] Ning Y, Yao M, Li Y, Song G, Liu Z, Li Q, et al. Integrated investigation on the nucleation and growing process of hydrate in W/O emulsion containing asphaltene. Chem Eng J 2023;454:140389. https://doi.org/10.1016/j. cei.2022.140389.
- [62] Leontaritis KJ, Mansoori GA. Asphaltene Flocculation During Oil Production and Processing: a Thermodynamic Colloidal Model. Soc Pet Eng AIME, SPE 1987: 149–58. https://doi.org/10.2523/16258-ms.
- [63] Feng Y, Li M, Han Y, Li Q, Lv X, Zhao J, et al. Gas hydrate nucleation and growth in a micro-reactor: effect of individual component separated from the crude oil in the South China Sea. Chem Eng J 2023;459:141483. https://doi.org/10.1016/j. cei.2023.141483.
- [64] Liu Y, Lv XF, Ma QL, Zhou SD, Shi BH, Du H, et al. Investigation on synergistic deposition of wax and hydrates in waxy water-in-oil (W/O) flow systems. Pet Sci 2022;19:1840–52. https://doi.org/10.1016/j.petsci.2022.04.004.
- [65] Liu Y, Wu C, Lv X, Du H, Ma Q, Wang C, et al. Hydrate growth and agglomeration in the presence of wax and anti-agglomerant: a morphology study and cohesive force measurement. Fuel 2023;342:127782. https://doi.org/10.1016/j. fiuel_2023.127782.
- [66] Andersen SI, Chandra MS, Chen J, Zeng BY, Zou F, Mapolelo M, et al. Detection and impact of carboxylic acids at the crude oil-water interface. Energy Fuel 2016;30: 4475–85. https://doi.org/10.1021/acs.energyfuels.5b02930.
- [67] Salmin DC, Delgado-Linares JG, Wu DT, Zerpa LE, Koh CA. Hydrate agglomeration in crude oil systems in which the asphaltene aggregation state is artificially modified. SPE J 2021;26:1189–99. https://doi.org/10.2118/204456-PA.
- [68] McLean JD, Kilpatrick PK. Effects of asphaltene aggregation in model heptanetoluene mixtures on stability of water-in-oil emulsions. J Colloid Interface Sci 1997;196:23–34. https://doi.org/10.1006/jcis.1997.5177.
- [69] Pickarts MA, Ravichandran S, Ismail NA, Stoner HM, Delgado-Linares J, Sloan ED, et al. Perspective on the oil-dominated gas hydrate plugging conceptual picture as applied to transient Shut-In/Restart. Fuel 2022;324:124606. https://doi.org/10.1016/j.fuel.2022.124606.